Structural Mapping of Adenosine Receptor Mutations: Ligand Binding and Signaling Mechanisms

Willem Jespers[1,3,4], Anke C. Schiedel[2], Laura H. Heitman[3], Robert M. Cooke[5], Lisa Kleene[2], Gerard J. P. van Westen[3], David E. Gloriam[4], Christa E. Müller[2], Eddy Sotelo[6] and Hugo Gutiérrez-de-Terán[1]*

[1] Department of Cell and Molecular Biology, Uppsala University, Biomedical Center, Box 596, SE-751 24, Uppsala, Sweden

[2] PharmaCenter Bonn, Pharmaceutical Institute, Pharmaceutical Chemistry I, An der Immenburg 4, 53121 Bonn, Germany

[3] Drug Discovery and Safety, Leiden/Amsterdam Center for Drug Research, Einsteinweg 55, 2333 CC, Leiden, Netherlands

[4] Department of Drug Design and Pharmacology, Universitetsparken 2, University of Copenhagen, Universitetsparken 2, 2100, Copenhagen, Denmark

[5] Heptares Therapeutics, Biopark, Broadwater Road, Welwyn Garden City, Hertfordshire, UK

[6] Centro Singular de Investigación en Química Biolóxica e Materiais Moleculares (CIQUS) and Departamento de Química Orgánica, Facultade de Farmacia. Universidade de Santiago de Compostela, 15782. Santiago de Compostela, Spain

* Correspondence: hugo.gutierrez@icm.uu.se (H. Gutiérrez-de-Terán)

Keywords: G protein-coupled receptor, Adenosine receptor, Mutagenesis, Chemical Modulation

Abstract

The four adenosine receptors, A_1, A_{2A}, A_{2B} and A_3, constitute a subfamily of G protein-coupled receptors (GPCRs) with exceptional foundations for structure-based ligand design. The vast amount of mutagenesis data, accumulated in the literature since the 1990s, has been recently supplemented with structural information, currently consisting of several inactive and active structures of the A_{2A} and inactive conformations of the A_1 adenosine receptor. We provide the first integrated view of the pharmacological, biochemical and structural data available for this receptor family, by mapping onto the relevant crystal structures all site-directed mutagenesis data, curated and deposited at the GPCR database (available through http://www.gpcrdb.org). This analysis provides novel insights into ligand binding, allosteric modulation, and signaling of the adenosine receptor family.

Adenosine receptors, a GPCR family with extensive structural information

G protein-coupled receptors (GPCRs, see Glossary) are an important class of membrane proteins targeted by approximately one third of the drugs currently on the market [1,2]. They are activated by a wide variety of signaling molecules of very different nature: from proteins or peptides (i.e chemokine receptors), to small neurotransmitters and neuromodulators including nucleosides and nucleotides [3]. The latter group is where we find the four receptors activated by adenosine, consisting of the A_1, A_{2A}, A_{2B} and A_3 **adenosine receptors** (ARs) [4]. They mediate central nervous system (CNS) depressant, anticonvulsant, sleep-promoting, antidiuretic, negative inotropic, negative chronotropic, anti-inflammatory, immunosuppressive and angiogenic effects, and are involved in the pathophysiology of cardiovascular and neurodegenerative diseases, as well as in cancer growth and immune responses [5,6]. The tremendous interest from both

academia and industry in ARs is in stark contrast to the low success of drug candidates in reaching the market. To date only one selective AR ligand, the A_{2A} **agonist** regadenoson, has gained FDA approval (as a coronary vasodilator used in cardiac imaging), while an **antagonist** of the same receptor, istradefylline, has been approved in Japan in combination with levodopa for the treatment of Parkinson's disease [7].

Since the cloning of ARs in the beginning of the 1990s, the tremendous efforts to characterize them has led to the accumulation of a substantial amount of experimental data. Decades of site-directed mutagenesis (SDM; Box 1) studies, in combination with pharmacological data and computational modeling, have paved the way for understanding receptor-ligand binding and activation signaling pathways. More recently, advances in membrane protein engineering and crystallography have sparked a surge of experimental GPCR structures [8], among which ARs have emerged as one of the most thoroughly characterized families: several structures are available for the inactive conformation of the human $A_{2A}AR$ bound to different chemotypes of orthosteric antagonists (Box 2) [9–11]. Some of these reveal allosteric sites, like the binding site for the negative **allosteric modulator** (NAM) sodium (Na^+) [12], or potential allosteric sites in the extracellular loop (EL) region [13]. Recently, the A_1AR has been crystallized in complex with xanthine antagonists [14,15]. In addition, active-like (agonist-bound) structures of the $A_{2A}AR$ have been obtained with several adenosine derivatives [16–18], lately complemented with the first fully active conformation bound to an engineered G protein fragment [19].

The current structural information is further supplemented by data obtained from additional, complementary techniques (Box 1). These include nuclear magnetic resonance (NMR) [20, 21]

or the mutagenesis/modeling combination known as biophysical mapping (BPM) [22], a technique recently employed to design $A_{2A}AR$ antagonists [23]. These different sources of experimental data can be integrated in computational models, which are used to elucidate the molecular determinants of ligand binding and receptor function [24]. In the ARs, protocols like **proteochemometrics** (PCM) [25] or **free energy perturbation** (FEP) [24,26] have successfully filled the gap between affinity and structural data (Box 1).

We herein review all the available mutagenesis data on the light of the structural information available for ARs. To do so, the existing SDM data was systematically collected from 80 individual publications and the resulting 2624 curated data points, of which 96% are from human receptors, were made available through the GPCRdb [27]. A comprehensive mapping of these data onto the available structural information provides an overview of ligand binding and activation events, which we present here in three sections: 1) Orthosteric ligand binding, 2) Allosteric modulation and 3) Receptor activation and G protein binding (Figure 1, Key Figure).

Orthosteric ligand binding

The common core scaffold of agonists and antagonists

Classical AR agonists and antagonists share a number of interactions within the orthosteric binding pocket, since they are derived of a similar planar heterocycle (Box 2), from where modifications can confer high affinity, selectivity and/or intrinsic activity (i.e. the ribose moiety). The crystal structures of the $A_{2A}AR$ confirmed that the central heterocycle of both agonists and antagonists resides in the same binding pocket, dominated by hydrogen bonds (H-bonds) with

the completely conserved N253^{6x55}(N/N/N/N) in all AR subtypes (see Box 3 for an explanation on residue numbering). The key role of this residue was suggested by early alanine scannings in different ARs, [22,28–32] in all cases abolishing ligand binding (Figure 2b) while retaining normal expression and basal activity levels [28]. The heterocyclic core is further stabilized by π–π stacking with F168^{45x52}(F/F/F/F) in the second extracellular loop (EL2), which could be replaced by another aromatic residue (tryptophan) with no significant changes in ligand binding affinities [28,33]. The neighboring residue, E169^{EL2}(E/E/E/V), is involved in ligand binding, through an H-bond in the scaffolds bearing an exocyclic amino group (Figure 2a and Box 2), while it can create a lid closing the binding site via a salt bridge interaction with H264^{EL3}(H/H/N/-) [34]. This double role explains why mutation to alanine completely abolishes binding of the agonist CGS21680 [35] and the antagonist ZM241385 [36], while binding is preserved upon a more conservative mutation to glutamine. Interestingly, the A$_{2A}$AR has been crystallized with and without this salt bridge linking EL2 and EL3, and in the A$_1$AR K265^{EL3}(K/A/G/P), might replace H264^{EL3} in this salt bridge. The role of this salt bridge in **ligand binding kinetics** is explained below.

Selectivity hotspots: mutagenesis suggestions confirmed by crystal structures

Deeper in the binding pocket, H250^{6x52} (H/H/H/S) stabilizes both agonists and antagonists, through interaction with the different modifications emerging from the core scaffold. This is in line with the abolished A$_{2A}$AR binding observed in the H250^{6x52}A mutant [30,32], while mutation to a bulky phenylalanine did not significantly affect antagonist binding (Figure 2b) [32,37]. The A$_3$AR has a serine in this position, which might explain why it is more tolerant towards larger substituents binding deep in the pocket. Another selectivity hotspot was recently

confirmed for the A_1AR, where $T270^{7x34}$(T/M/M/L), a previously proposed hotspot for A_1AR interspecies selectivity [38], accommodates cycloalkylic groups at the C8-position of xanthines, characteristic of A_1-selective xanthine derivatives (Figure 2c) [14,15]. Consequently, a $M270T^{7x34}$ mutant $A_{2A}AR$ showed increased affinity for A_1 selective ligands, whose affinity was correspondingly reduced in the inverse mutant ($T270M^{7x34}$ mutant of the A_1AR [14,15]). The comparison of A_1AR and $A_{2A}AR$ inactive structures highlighted another difference leading to antagonist selectivity. The N1-substituent of the xanthine derivative PSB-36 occupies a narrow cavity between TM3, TM5 and TM6 in the A_1AR, which is not present in the $A_{2A}AR$. Consequently, PSB-36 is forced to sit in an alternative, less-favorable position [15].

Triggering receptor activation: residues involved in agonist recognition

The triad formed by $E13^{1x39}$ (E/E/E/E) – $S277^{7x42}$ (T/S/S/S) – $H278^{7x43}$ (H/H/H/H), together with $T88^{3x36}$ (T/T/T/T) and $H250^{6x52}$ (H/H/H/S), constitute the main binding site for the ribose moiety in (full) agonists (Figure 2d). This triad was proposed in the early nineties as an important structural feature for AR activation [39], further supported by experiments using a 'neoceptor' approach [40,41] (Box 3). The $E13^{1x39}$ – $H278^{7x43}$ interaction is present in all agonist crystal structures, stabilizing the conformation of $H278^{7x43}$ required to form an H-bond with the ribose moiety. Consequently, mutations of $E13A^{1x39}$ reduce the **potency** of full agonists, but interestingly not of non-nucleoside **partial agonists** [28]. Using molecular dynamics (MD) simulations, Rodríguez et al. showed that this interaction was not only less stable in the absence of a ligand, but also dependent on the protonation state of the residues involved, which might be altered by the presence of full agonists [42]. Removal of either of the two histidine sidechains in

the binding site in the H250A^{6x52} [30,32] and H278A^{7x43} [32] mutants strongly decreased agonist potency and binding, and also reduced antagonist binding.

Mutation of other polar sidechains coordinating the ribose in the A$_{2A}$AR (S277A^{7x42} [32] and T88A$^{3.36}$ [43]) reduced agonist potency, but increased antagonist binding and the potency of the partial agonist LUF5834 [28]. Crystal structures of agonist-bound A$_{2A}$AR show a direct interaction between NECA and T88^{3x36} through the amide in position 5' of the ribose, which is not present in adenosine. This could explain why NECA is more sensitive to the T88A$^{3.36}$ mutation and has a higher affinity than adenosine for the A$_{2A}$AR [43–45]. Mutations of the polar sidechain at position 7x42 have a drastic effect on agonist binding, as seen in alanine mutants in the A$_{2B}$AR (S279A^{7x42}) [46] and the A$_1$AR (T277A^{7x42}) [47–49]. Additionally, the inactive A$_{2A}$ StaR ('stabilized receptors'; Box 1) contains alanine mutations of T88$^{3.36}$ and S277^{7x42} [50], while antagonists crystalized with the wild-type (wt) receptor do not show interactions with these residues, all of which points to a role of these polar sidechains in attaining a fully active conformation. Interestingly, the same mutants have negligible or even positive effects on the potency and/or efficacy of partial agonists at the A$_1$ [47–49] and A$_{2A}$ ARs [28].

Mutations on the orthosteric site, which represent 80% of the collected mutational data on ARs, have been characterized in more detail than the mutations on the allosteric or G protein sites described in the next sections. Indeed, *In silico* site-directed mutagenesis simulations of several A$_{2A}$AR orthosteric-site mutants (Box 1) provided a nice complement to the structural analysis of static crystal structures discussed above, revealing non-evident effects like water-mediated interactions or the role of mutations which are not in direct contact with the ligand [24,26].

The extracellular region: Ligand kinetics and receptor architecture

Mutations in the ELs do not only influence binding of orthosteric ligands, but may also play a role in ligand kinetics. In addition, this region plays a structural role through a series of cysteine bridges, and has been related to selectivity among certain receptor subtypes. Finally, mutational studies and lately crystal structures [11] suggest that this region might be the binding site of allosteric modulators, in analogy to other GPCRs [51]. Here we will discuss the mutational data of the EL region in ARs.

Residues that govern the kinetics of ligand binding

Ligand binding kinetics governs the **residence time** of a drug, which has deep implications on its clinical **efficacy** [52]. The kinetics of ligand binding in adenosine receptors has been demonstrated to be extremely variable, as recently examined by SDM and other methods [53]. Residues distant from the **orthosteric site** can influence the kinetics of ligand binding without altering the binding affinity constant (K_i). For instance, the k_{on} and k_{off} values ZM241385 on StaR versus wt receptors are significantly slower, but the binding affinity remains unaltered [54]. Other point mutations located in the binding site [L85A^{3x33}(L/L/L/L), Y271A^{7x35}(Y/Y/N/Y), and N181A^{5x43}(N/N/N/S)], on the other hand, simultaneously increased the k_{off} and decreased the binding affinity of the antagonist ZM241385 [22]. Mutations of residues located in the EL region of the A$_{2A}$AR, either increased [E169Q^{EL2} (E/E/E/V), H264A^{EL3}(H/H/Q/V), and T256A^{6x58}(T/T/T/I)] or decreased [I66A^{2x63}(I/I/I/V), S67A^{2x64}(N/S/S/S), K153A^{EL2}(W/K/C/R), and L267A^{7x31}(S/L/K/Q)] the k_{off} of ZM241385 [36], while its affinity was minimally affected.

This led to the conclusion that these residues should play a role in the dissociation pathway of ZM241385. Recent mutagenesis, crystal structures and MD simulations confirmed that breaking the salt bridge between E169[EL2], H264[EL3] (supported by polar interactions with T256[6x58]) is crucial in the dissociation of ZM241385 [36,55], as previously indicated by MD simulations of A_{2A} and A_{2B} receptors [42]. The stabilization of the salt bridge between E169[EL2] and the positively charged H264[EL3] should be considered in the design of $A_{2A}R$ antagonists with long residence time.

Architecture and stability of the variable EL2 region

The extracellular region - especially EL2 - differs within the AR family in terms of sequence length, composition and even tertiary structure (Figure 3b) [14,15]. The existence of cysteine bridges, which play an important role in the architecture and stability of the EL2, is variable between ARs. The cysteine bridge formed between C77[3x25](C/C/C/C) - C166[45x50] (C/C/C/C) is a highly conserved motif in class A GPCRs (87%) shared amongst all ARs [27] (Figure 3b). Serine mutations of one of these cysteines abolished ligand binding in the A_1 [56] and A_{2B} ARs [57], but in the $A_{2A}AR$ only resulted in reduced potency or affinity of small agonists (e.g. NECA, adenosine), whilst having no effect on larger 2-substituted adenosine derivatives (e.g. CGS21680) [51]. The reduced effect on this receptor could be understood with the first $A_{2A}AR$ crystal structures, revealing additional disulfide bridges that reinforce the architecture of EL2 due to two extra cysteines in this loop. Serine mutations of these cysteine residues [C146[EL2](L/C/K/K) and C159[EL2](M/C/G/S)] resulted in a lower potency of adenosine, but did not alter the potency of NECA and CGS21680. On the contrary, serine mutations in the $A_{2B}AR$ of the three cysteine residues present in EL2 [C154[EL2](W/K/C/R), C166[EL2] (K/A/C/-), C167[EL2] (-

9

/-/C/-)] did not affect ligand binding, indicating that they are not involved in disulfide bond formation [57]. Finally, the dynamics of the EL region might play a role in the allosteric modulation of ARs, which we will explain in the next section.

Sites for allosteric modulation in ARs

Allosteric modulation of GPCRs is gaining acceptance as a new approach for drug development, since allosteric ligands typically display higher target selectivity compared to orthosteric ligands [3,58]. In ARs, two distinct receptor regions have been revealed as sites for allosteric modulation (Figure 3): the EL2 region and the sodium binding pocket.

The EL2 as an allosteric region

The role of the extracellular loops in receptor structure and dynamics might explain why this region has been identified as a site for the binding of both positive (PAM) and negative (NAM) allosteric modulators. The A_{2A}-selective agonist CGS21680, as well as other non-selective agonists, showed an increased efficacy in a chimeric $A_{2B}AR$ receptor containing the EL2 of the $A_{2A}AR$ in comparison to the wt $A_{2B}AR$ [59,60]. These results suggest an allosteric control of EL2, since the increased agonist efficacies can be explained by the role of this loop in stabilizing agonist-bound receptor conformations [59]. Moreover, ligand selectivity may be achieved - probably by an indirect effect - in extracellular regions far away from the ligand binding pocket [61–63]. Recent results on the A_1AR provide additional evidence to the idea that ARs can be activated by positive allosteric modulators binding to the EL regions [64,65]. These insights have

been recently complemented by the observation of a potential allosteric pocket in a recently published antagonist-bound $A_{2A}AR$ structure [13].

Allosteric modulation by sodium ions and amilorides

Sodium ions down-regulate the pharmacological response of GPCRs, including the $A_{2A}AR$ [66]. The 1.8 Å resolution crystal structure of the inactive $A_{2A}AR$ in complex with ZM241385 proved the presence of a previously predicted sodium ion binding site formed by several GPCR-conserved residues, namely $D52^{2x50}$ (D/D/D/D), $S91^{3x39}$ (S/S/S/S), $W246^{6x48}$ (W/W/W/W), $N280^{7x45}$ (N/N/N/N) and $N284^{7x49}$ (N/N/N/N) (Figure 3d) [12]. This finding was followed by SDM and biophysical characterization of this pocket, combined with MD simulations, which revealed a mechanism of allosteric control where sodium specifically stabilizes the inactive conformation of the receptor [67,68]. Upon agonist binding, the sodium binding site collapses due to a concerted movement of several residues situated in TM3, TM6 and TM7. In particular, an H-bond is formed between the backbone oxygen in $N284^{7x49}$, part of the highly conserved NPxxY motif, and $D52^{2x50}$, which is one of the highest conserved residues amongst the entire family of GPCRs [27,69]. Accordingly, alanine mutations of both $N284^{7x49}$ [67,70] and $D52^{2x50}$ [67,71] had little effect on antagonist or agonist binding but completely abolished receptor activation. A series of MD simulations of the β_2-adrenergic receptor, mapped onto the $A_{2A}AR$ crystal structures, concluded that the protonation state of $D52^{2x50}$ changes during the activation pathway from an inactive, deprotonated, to an active, protonated state. In this scenario, $S91^{3x39}$ would play a regulatory role in the protonation of $D52^{2x50}$, as mutations to alanine in A_1 and A_{2A} ARs increase their basal activities [44,67,69]. In the active-like state, the backbone interaction

between $D52^{2x50}$ and $N284^{7x49}$ causes a helix bulge in TM7, leading to conformational rearrangements related to receptor activation as discussed in the next section.

Another conformational change is initiated by the movement of residues $W246^{6x48}$ and $F242^{6x44}$, which propagates to an outward shift of TM6 as observed in agonist-bound and fully activated structures (Figure 3c). This movement might be blocked by amiloride and derivatives, which are NAMs predicted to bind to the sodium site [67], which is in line with data showing that $F242A^{6x44}$ mutations increase the thermostability of agonist-bound $A_{2A}AR$ [50]. Tryptophan $W246^{6x48}$, previously coined as the 'toggle switch' [9], forms a bulky lining separating the orthosteric site from the sodium binding site. Mutation to alanine did not alter agonist binding to the A_3AR, but receptor function was completely lost [30,71,72]. Similarly, on the $A_{2A}AR$ the corresponding $W246^{6x48}A$ mutant reduced the efficacy of full agonists, whereas the activity of partial agonists was slightly increased [28,46,67,73].

Mutations in the sodium pocket affect amilorides in a different way compared to sodium. Allosteric modulation by sodium was completely abolished in $D52A^{2x50}$ and $N284A^{7x49}$ receptor mutants, but the latter showed increased affinity for amilorides. The interpretation, supported by MD simulations, was that the positively charged guanidinium group of amiloride would form a salt bridge with $D52^{2x50}$, while $N284^{7x49}$, $N280^{7x45}$, and $W246^{6x48}$ would make suboptimal interactions with amilorides. Additionally, $W246A^{6x48}$ has been shown to increase the competitive behavior of amilorides in radioligand binding assays with ZM241385, due to an increased penetration of 5'-substituted amilorides into the orthosteric binding site in the mutant receptor [74].

Receptor signaling and G protein binding

The intracellular side of the TM bundle is more conserved within the GPCR superfamily than the extracellular domain [2]. This region undergoes the most pronounced conformational changes upon receptor activation and is implicated in the binding of the intracellular G-protein. Four motifs play a major role here (Figure 4): NPxxY in TM7, the DRY motif (TM3), the ionic lock and the TDY triad, as observed in the G protein-bound crystal structure [19].

The TM7 NPxxY motif

This motif is located in TM7 and contains $N284^{7x49}$, which has been discussed above as part of the sodium binding site, and is the center of the helix bulge observed in $A_{2A}AR$ active-like structures (Figure 3d). Residue $Y288^{7x53}$ experiences an upward movement and undergoes an H-bond interaction with $Y197^{5x58}$ (Y/Y/Y/Y) in the G protein-bound structure (Figure 4b). These pair of tyrosines is considered as a possible activation switch, based on their high conservation in class A GPCRs [27] and their specific interaction in the G protein-bound state, while the sidechain of $Y197^{5x58}$ was shown to flip out into the membrane in $A_{2A}AR$ agonist-bound crystal structures [16–18] (Figure 4b). The $Y282F^{7x53}$ mutation in the A_3AR resulted in a nearly 30-fold reduction in potency for Cl-IB-MECA, but did not alter basal activities [75]. In the $A_{2B}AR$, the $Y197S/N^{5x58}$ mutations, which maintain the polarity of the wt tyrosine, led to an increase in constitutive activity [62]. To fully understand the role of the $Y197^{5x58}$ - $Y288^{7x53}$ switch in AR activation, mutations to alanine and phenylalanine would be of particular interest.

The TM3 DRY motif

The GPCR conserved DRY (D101$^{3.49}$ (D/D/D/D) - R102$^{3.50}$ (R/R/R/R) – Y103$^{3.51}$ (Y/Y/Y/Y)) motif in TM3 binds the C-terminus of the G protein in the fully activated A$_{2A}$AR. R102A$^{3.50}$ moves towards Y197^{5x58}, in analogy to the fully-active β$_2$ structure, to allow the G protein to move in, and undergoes intensive van der Waals interactions with Y391 in the mini G$_s$- A$_{2A}$AR bound structure [19]. In a mutational study on the A$_{2B}$AR addressed to investigate its selectivity for G proteins, it was found that R102A$^{3.50}$ maintained potency and maximum response close to the wt receptor for the G$_{αs}$ subtype, but lost potency for seven other subtypes [76]. In the A$_3$AR, mutations R102A$^{3.50}$ and R102K$^{3.50}$ led to constitutively active receptors [75]. Interestingly, two structural motifs, the ionic lock (Figure 4c) and the TDY triad (Figure 4d), keep R102$^{3.50}$ locked in the conformation observed in inactive and agonist-bound structures of A$_{2A}$AR, as opposed to the corresponding fully-active, mini G$_s$- A$_{2A}$AR crystal structure.

The ionic lock

The salt bridge formed between E228^{6x30} (E/E/E/E) and R102^{3x50} (R/R/R/R), also called the ionic lock, is proposed to be an important factor in the deactivation of the receptor. It is present in several but not all A$_{2A}$AR inactive crystal structures [10]. No mutation data is available for residue E228^{6x30} in ARs, but other experimental work points towards a regulatory role of this salt-bridge in receptor activation. In particular, NMR based studies of the A$_{2A}$AR show a rapid interchange (low millisecond timescale) of two antagonist states, associated with ionic lock formation [20]. In analogy to the case of the β$_2$ adrenergic receptor, MD simulations of the A$_{2A}$AR, starting from a conformation where the ionic lock was not present, showed a rapid formation (10 - 15 ns timescale) and highly stable (100ns) ionic lock interaction [42,77]. A

recent $A_{2A}AR$ crystal structure revealed an interaction between $E228^{6x30}$ and $R107^{3x55}$ (K/R/C/K) [13], which together with the thermostabilizing effect of the $R107A^{3x55}$ mutant [10], suggests a role of this residue against the formation of the ionic lock.

The TDY triad

Residues $T41^{2x39}$ (T/T/T/T) – $D101^{3x49}$ (D/D/D/D) (<u>D</u>RY) – $Y112^{34x53}$ (Y/Y/Y/Y) form a triad fully conserved amongst all AR subtypes and some other class A families (e.g. β-adrenergic and dopamine receptors) [27]. This triad has previously been suggested to be involved in a network of polar interactions stabilizing the ionic lock [42]. The $T41^{2x39}A$ mutation has been shown to produce constitutively active $A_{2B}ARs$ [29,78]. In the A_3AR, mutations of $D107^{3x49}$ to asparagine, lysine and arginine did not significantly alter the basal activities of the receptor or the potency of agonists [75]. No mutational data for $Y112^{34x53}$ is available for ARs. Notably, the structural differences of the corresponding TDY triad in the different conformations of the β₂ adrenergic receptor are more pronounced than in the $A_{2A}AR$. In all β₂ structures the IL2 is disordered except for the fully activated structure, where the region forms an-alpha helix. This results in a H-bond between Y^{34x53} and D^{3x49}, possibly altering the salt bridge strength between R^{3x50} and D^{3x49}. In the $A_{2A}AR$, the IL2 is consistently found in an alpha helical conformation, and the shape of the TDY triad remains the same. Additional mutagenesis experiments are needed to confirm a possible regulatory role of this triad in the activation of ARs and other class A GPCRs.

Concluding Remarks

The effects of point mutations of the four ARs on ligand binding affinities, functional potencies and efficacies constitute a valuable source of pharmacological information. We analyzed the

existing data and mapped it on the collection of available AR crystal structures, allowing for a comprehension of receptor-ligand interactions and receptor activation outstanding within the GPCR families. A majority of the mutational data collected refers to orthosteric ligand binding, where combinations of SDM and crystal structures led to the design of AR antagonists [79], and novel computational protocols have provided with detailed energetic descriptions of ligand binding. Still, some issues remain unsolved with regard to ligand optimization, such as achieving better selectivity ratios or attaining an agonist functional response on ligands lacking a ribose moiety, though recent advances in this regard are promising [80]. Allosteric modulation is a promising pharmacological strategy to overcome some of these issues, but while there is indirect evidence pointing to the location of allosteric sites on the EL region, a crystal structure with an allosteric modulator is still lacking. The kinetic characterization of ligand binding is an emerging area, though not yet fully understood, where new mutational and structural data could be particularly helpful. Finally, the crystal structures of $A_{2A}AR$ provide a complete landscape of end-point receptor conformational states, complemented with mutational data that points to specific activation switches, but additional mutations and ligands that stabilize intermediate conformational states are needed to fully understand the activation mechanism. These and other key issues in the field are collected in the Outstanding Questions. Our analysis shows that the ARs constitute a family of GPCRs with an exceptional knowledge base of structural, biochemical and pharmacological data, which configures a useful and dynamic map to design orthosteric and allosteric modulators, and envisage molecular switches involved in receptor activation and signaling.

Acknowledgement

16

Conflict of Interest. The authors declare that they have no conflict of interest

Box 1: Experimental and computational methods to investigate binding and signaling events in ARs.

- Site-directed mutagenesis: A classical molecular biology method, where a single mutation is engineered in the DNA sequence codifying the receptor, to further investigate receptor structural or biological properties. Ligand binding affinities are measured in terms of their ability to competitively displace the radioligand, yielding ligand affinity ratios between the receptor mutant and wild-type (wt) variants. An analogous comparison can be made in functional assays to evaluate the effect on the potency or efficacy of agonists.

- Neoceptor: An approach to investigate the (direct) role of residues in ligand binding, where the (fractional) charges of both ligand and protein are simultaneously reversed to investigate the (direct) role of residues in ligand binding. It was first introduced by Jacobson *et al*. into the AR field and has since been used in several examples [40,41].

- Thermostabilization: A mutagenesis strategy to increase the thermostability of GPCRs, leading to the so-called Stabilized Receptors (StaRs). This method has been patented and applied on the $A_{2A}AR$, resulting in A_{2A}-StaR2 that contained 8 mutations, which stabilized the antagonist state of the receptor: $A54L^{2x52}$(A/A/A/A), $T88A^{3x36}$(T/T/T/T), $R107A^{3x55}$(K/R/C/K), $K122A^{4x43}$(A/K/R/W), $N154A^{EL2}$(A/N/T/N), $L235A^{6x37}$(L/L/L/L) $V239A^{6x41}$(L/V/V/L), and $S277A^{7x42}$(T/S/S/S)[54]. Similarly, the inactive A_1-StaR was constructed containing 6 mutations: $A57L^{2x52}$, $T91A^{3x36}$, $Y205A^{5x63}$(Y/L/L/Y), $L236A^{6x37}$, $L240A^{6x41}$ and $T277A^{7x42}$.

- Biophysical mapping: Starting from a StaR (see above), additional single mutations are added at positions that could be involved in small molecule interactions. The StaR and a panel of binding site mutants are captured onto Biacore chips to enable characterization of

ligand binding using surface plasmon resonance (SPR) measurement. A matrix of binding data for a set of ligands versus each active site mutation is then generated, providing specific affinity and kinetic information (K_d, k_{on}, and k_{off}) of receptor-ligand interactions. This proprietary method has been used in the discovery of $A_{2A}AR$ antagonists [11,22].

- NMR: Classical NMR experiments recently revealed the conformational selection of ligands for certain receptor states [20], while the NMR determination of interligand NOEs for pharmacophore mapping (INPHARMA) was employed to obtain information on ligand poses inside the binding site of the $A_{2A}AR$ reconstituted into nanodiscs [52]

- *In silico* site-directed mutagenesis. This protocol, based on free energy perturbation of residue sidechains, can be used to identify the molecular interactions that are gained or lost as a result of the point mutation. Since the corresponding shifts in ligand binding free energy are related to molecular interactions, as demonstrated on 34 of the $A_{2A}AR$ mutants described in this review [24,26].

Box 2: Ligands co-crystallized with adenosine receptors

- The chemical nature and functional behavior of the ligands co-crystallized with the A_{2A} and A_1 ARs is variable. Still, most of the agonists and antagonists are derivatives or analogs of purine, a planar heterocycle (imidazo[4,5-*d*]pyrimidine, blue sub-structure in Figure I), present in the endogenous agonist adenosine. This allows some conserved interactions between receptor and both agonist and antagonist, like the hydrogen bonds with $N253^{6.55}$ (N/N/N/N) (Box 3 explains residue nomenclature), due to the chemical motif denoted with a red square on each structure.

- Full agonists (upper row, Figure I) are clearly differentiated by bearing a sugar moiety at position 9, some of which contain an ethylamido modification at C4' of the ribose instead of a hydroxymethylene group (NECA, UK432097 and CGS21680). The amino group at position 6 of the purine ring may bear a bulky substituent (UK432097), while different substituents are allowed at position 2 (UK432097 and CGS21680).

- Most antagonists (Figure I, second row) also contain a purine core or an analogous heterobicycle (blue) as is the case for xanthine derivatives (caffeine, XAC, DU172 and PSB-36, the last two co-crystallized with the A_1AR) or the azapurine present in the triazolotriazine ZM241385. The triazine derivatives T4G, T4E and the aminotriazole 8D1 are exceptions bearing structurally simple, monocyclic cores. Other antagonists have been described for ARs, but we here focus on those for which there is mutational and structural data.

Box 3: Generic residue numbering

All residues and their mutations have been numbered according to the following scheme:

$$A000B^{Tx00}(C/D/E/F)$$

Where:

- A = the wild-type residue.

- 000 = the residue number of the mutated residue, this number corresponds with the residue numbering of the receptor under investigation.

- B = the mutated residue, if no mutation is given this entry is left blank.

- ^{Tx00} = the GPCRdb numbering scheme, which is a structure-based update of the Ballesteros-Weinstein (B-W) numbering scheme. T represents the transmembrane helix number and 00 the correlative residue number. The latter starts at the most conserved topological position in each helix, which is numbered 50. Here we adopt the last modifications to this numbering scheme, accounting for structural kinks and bulges in the alignment and numbering [81]. Residues in an inter- or extracellular domain of the receptor are represented using ^{00x00}, where the first two numbers depict the two transmembrane domains before and after the inter- or extracellular domain. If the residue position is not conserved, which is mostly the case in extra and intracellular loops and termini, no number is assigned and instead it is indicated the loop region where it belongs (EL1-IL3).

- C/D/E/F = the residue type in adenosine A_1, A_{2A}, A_{2B} and A_3 respectively, which will be given once in a paragraph.

The topological domains were classified as TM1-7 for the seven transmembrane helices, H8 (the C-terminal α helix), EL1-3 for the extracellular and IL1-3 to the intracellular loops.

References

1   Santos, R. *et al*. (2016) A comprehensive map of molecular drug targets. *Nat*. *Rev*. *Drug Discov*. 16, 19–34

2   Hauser, A.S. *et al*. (2017) Trends in GPCR drug discovery: new agents, targets and indications. *Nat Rev Drug Discov, Accept*. DOI: 10.1038/nrd.2017.178

3   Venkatakrishnan, a J. *et al*. (2013) Molecular signatures of G-protein-coupled receptors. *Nature* 494, 185–194

4   Fredholm, B.B. *et al*. (2011) International Union of Basic and Clinical Pharmacology. LXXXI. Nomenclature and classification of adenosine receptors-an update. *Pharmacol*. *Rev*. 63, 1–34

5   Haskó, G. *et al*. (2008) Adenosine receptors: therapeutic aspects for inflammatory and immune diseases. *Nat*. *Rev*. *Drug Discov*. 7, 759–770

6   Leone, R.D. *et al*. $A_{2A}R$ antagonists: Next generation checkpoint blockade for cancer immunotherapy. *Comput*. *Struc*. *Biotechnol*. *J*., 13. (2015) , 265–272

7   Chen, J.-F. *et al*. (2013) Adenosine receptors as drug targets--what are the challenges? *Nat*. *Rev*. *Drug Discov*. 12, 265–286

8   Katritch, V. *et al*. (2013) Structure-function of the G protein-coupled receptor superfamily. *Annu*. *Rev*. *Pharmacol*. *Toxicol*. 53, 531–556

9   Jaakola, V.-P. *et al*. (2008) The 2.6 angstrom crystal structure of a human A_{2A} adenosine receptor bound to an antagonist. *Science* 322, 1211–1217

10   Doré, A.S. *et al*. (2011) Structure of the adenosine A_{2A} receptor in complex with ZM241385 and the xanthines XAC and caffeine. *Structure* 19, 1283–1293

11   Congreve, M. *et al*. (2012) Discovery of 1,2,4-Triazine Derivatives as Adenosine A_{2A}

antagonists using structure based drug design. *J. Med. Chem.* 55, 1898–1903

12   Liu, W. *et al.* (2012) Structural basis for allosteric regulation of GPCRs by sodium ions. *Science* 337, 232–236

13   Sun, B. *et al.* (2017) Crystal structure of the adenosine A_{2A} receptor bound to an antagonist reveals a potential allosteric pocket. *Proc. Natl. Acad. Sci. U. S. A.* 114, 2066–2071

14   Glukhova, A. *et al.* (2017) Structure of the adenosine A_1 receptor reveals the basis for subtype selectivity. *Cell* 168, 867–877

15   Cheng, R.K.Y. *et al.* (2017) Structures of human A_1 and A_{2A} adenosine receptors with xanthines reveal determinants of selectivity. *Structure* 25, 1275–1285

16   Lebon, G. *et al.* (2011) Agonist-bound adenosine A_{2A} receptor structures reveal common features of GPCR activation. *Nature* 474, 521–525

17   Xu, F. *et al.* (2011) Structure of an agonist-bound human A_{2A} adenosine receptor. *Science* 332, 322–327

18   Lebon, G. *et al.* (2015) Molecular determinants of CGS21680 binding to the human adenosine A_{2A} receptor. *Mol. Pharmacol.* 87, 907–915

19   Carpenter, B. *et al.* (2016) Structure of the adenosine A_{2A} receptor bound to an engineered G protein. *Nature* 536, 104–107

20   Ye, L. *et al.* (2016) Activation of the A_{2A} adenosine G-protein-coupled receptor by conformational selection. *Nature* 533, 265–268

21   Fredriksson, K. *et al.* (2017) Nanodiscs for INPHARMA NMR characterization of GPCRs: Ligand binding to the human A_{2A} adenosine receptor. *Angew. Chemie Int. Ed.* 56, 5750–5754

22   Zhukov, A. *et al*. (2011) Biophysical mapping of the adenosine A$_{2A}$ receptor. *J. Med. Chem*. 54, 4312–4323

23   Langmead, C.J. *et al*. (2012) Identification of novel adenosine A$_{2A}$ receptor antagonists by virtual screening. *J. Med. Chem*. 55, 1904–1909

24   Gutiérrez-de-Terán, H. *et al*. (2017) Structure-based rational design of adenosine receptor ligands. *Curr. Top. Med. Chem*. 17, 40–58

25   Van Westen, G.J.P. *et al*. (2012) Identifying novel adenosine receptor ligands by simultaneous proteochemometric modeling of rat and human bioactivity data. *J. Med. Chem*. 55, 7010–7020

26   Keränen, H. *et al*. (2015) Free energy calculations of A$_{2A}$ adenosine receptor mutation effects on agonist binding. *Chem. Commun*. 51, 3522–3525

27   Isberg, V. *et al*. (2016) GPCRdb: an information system for G protein-coupled receptors. *Nucleic Acids Res*. 44, D356–D364

28   Lane, J.R. *et al*. (2012) A novel nonribose agonist, LUF5834, engages residues that are distinct from those of adenosine-like ligands to activate the adenosine A$_{2A}$ receptor. *Mol. Pharmacol*. 81, 475–487

29   Li, Q. *et al*. (2007) ZM241385, DPCPX, MRS1706 are inverse agonists with different relative intrinsic efficacies on constitutively active mutants of the human adenosine A$_{2B}$ receptor. *J. Pharmacol. Exp. Ther*. 320, 637–645

30   Gao, Z. *et al*. (2002) Identification by Site-directed Mutagenesis of Residues Involved in Ligand Recognition and Activation of the Human A$_3$ Adenosine Receptor. *J. Biol. Chem*. 277, 19056–19063

31   May, L.T. *et al*. (2011) Allosteric interactions across native adenosine A$_3$ receptor

homodimers: quantification using single-cell ligand-binding kinetics. *FASEB J.* 25, 3465–3476

32   Kim, J. *et al.* (1995) Site-directed Mutagenesis Identifies Residues Involved in Ligand Recognition in the Human A_{2A} Adenosine Receptor. *J. Biol. Chem.*, 270, 13987–13997

33   Jaakola, V.-P. *et al.* (2010) Ligand binding and subtype selectivity of the human A_{2A} adenosine receptor: identification and characterization of essential amino acid residues. *J. Biol. Chem.* 285, 13032–13044

34   Wheatley, M. *et al.* (2012) Lifting the lid on GPCRs: the role of extracellular loops. *Br. J. Pharmacol.* 165, 1688–1703

35   Kim, J. *et al.* (1996) Glutamate residues in the second extracellular loop of the human A_{2A} adenosine receptor are required for ligand recognition. *Mol. Pharmacol.* 49, 683–691

36   Guo, D. *et al.* (2016) Molecular basis of ligand dissociation from the adenosine A_{2A} receptor. *Mol. Pharmacol.* 89, 485–491

37   Jiang, Q. *et al.* (1997) Mutagenesis reveals structure-activity parallels between human A_{2A} adenosine receptors and biogenic amine G protein-coupled receptors. *J. Med. Chem.* 40, 2588–2595

38   Tucker, A.L. *et al.* (1994) A_1 adenosine receptors. Two amino acids are responsible for species differences in ligand recognition. *J. Biol. Chem.* 269, 27900–27906

39   IJzerman, A.P. *et al.* (1996) Site-directed mutagenesis of the human adenosine A_{2A} receptor. Critical involvement of Glu13 in agonist recognition. *Eur. J. Pharmacol.* 310, 269–272

40   Gao, Z.G. *et al.* (2006) Orthogonal activation of the reengineered A_3 adenosine receptor (neoceptor) using tailored nucleoside agonists. *J. Med. Chem.* 49, 2689–2702

41   Zeevaart, J.G. *et al*. (2001) Neoceptor concept based on molecular complementarity in GPCRs: A mutant adenosine A_3 receptor with selectively enhanced affinity for amine-modified nucleosides. *J. Med. Chem.* 130, 9492–9499

42   Rodríguez, D. *et al*. (2011) Molecular dynamics simulations reveal insights into key structural elements of adenosine receptors. *Biochemistry* 50, 4194–4208

43   Bertheleme, N. *et al*. (2013) Loss of constitutive activity is correlated with increased thermostability of the human adenosine A_{2A} receptor. *Br. J. Pharmacol.* 169, 988–998

44   Jiang, Q. *et al*. (1996) Hydrophilic side chains in the third and seventh transmembrane helical domains of human A_{2A} adenosine receptors are required for ligand recognition. *Mol. Pharmacol.* 50, 512–521

45   Magnani, F. *et al*. (2008) Co-evolving stability and conformational homogeneity of the human adenosine A_{2A} receptor. *Proc. Natl. Acad. Sci. U.S.A.* 105, 10744–10749

46   Thimm, D. *et al*. (2013) Ligand-specific binding and activation of the human adenosine A_{2B} receptor. *Biochemistry* 52, 726–740

47   Townsend-Nicholson, A. and Schofield, P.R. (1994) A threonine residue in the seventh transmembrane domain of the human A_1 adenosine receptor mediates specific agonist binding. *J. Biol. Chem.* 269, 2373–2376

48   Dalpiaz, A. *et al*. (1998) Thermodynamics of full agonist, partial agonist, and antagonist binding to wild-type and mutant adenosine A_1 receptors. *Biochem. Pharmacol.* 56, 1437–1445

49   Kourounakis, A. *et al*. (2001) Differential effects of the allosteric enhancer (2-amino-4,5-dimethyl-trienyl)[3-(trifluoromethyl) phenyl]methanone (PD81,723) on agonist and antagonist binding and function at the human wild-type and a mutant (T277A) adenosine

A$_1$ receptor. *Biochem. Pharmacol.* 61, 137–144

50   Lebon, G. *et al.* (2011) Thermostabilisation of an agonist-bound conformation of the

human adenosine A$_{2A}$ receptor. *J. Mol. Biol.* 409, 298–310

51   De Filippo, E. *et al.* (2016) Role of extracellular cysteine residues in the adenosine A$_{2A}$

receptor. *Purinergic Signal.* 12, 313–329

52   Copeland, R.A. (2015) The drug–target residence time model: a 10-year retrospective.

Nat. Rev. Drug Discov. 15, 87–95

53   Guo, D. *et al.* (2017) Kinetic aspects of the interaction between ligand and G protein-

coupled receptor: The case of the adenosine receptors. *Chem. Rev.* 117, 38–66

54   Robertson, N. *et al.* (2011) The properties of thermostabilised G protein-coupled receptors

(StaRs) and their use in drug discovery. *Neuropharmacol.* 60, 36–44

55   Segala, E. *et al.* (2016) Controlling the dissociation of ligands from the adenosine A$_{2A}$

receptor through modulation of salt bridge strength. *J. Med. Chem.* 59, 6470–6479

56   Scholl, D.J. and Wells, J.N. (2000) Serine and alanine mutagenesis of the nine native

cysteine residues of the human A$_1$ adenosine receptor. *Biochem. Pharmacol.* 60, 1647–

1654

57   Schiedel, A.C. *et al.* (2011) The four cysteine residues in the second extracellular loop of

the human adenosine A$_{2B}$ receptor: Role in ligand binding and receptor function. *Biochem.

Pharmacol.* 82, 389–399

58   Shonberg, J. *et al.* (2014) GPCR crystal structures: Medicinal chemistry in the pocket.

Bioorg. Med. Chem. 23, 3880–3906

59   Seibt, B.F. *et al.* (2013) The second extracellular loop of GPCRs determines subtype-

selectivity and controls efficacy as evidenced by loop exchange study at A$_2$ adenosine

receptors. *Biochem*. *Pharmacol*. 85, 1317–1329

60   Olahs, M.E. *et al*. (1994) Role of the second extracellular loop of adenosine receptors in

agonist and Antagonist binding. *J*. *Biol*. *Chem*. 269, 24692–24698

61   Kennedy, D.P. *et al*. (2014) The second extracellular loop of the adenosine A_1 receptor

mediates activity of allosteric enhancerss. *Mol*. *Pharmacol*. 85, 301–309

62   Peeters, M.C. *et al*. (2012) Three "hotspots" important for adenosine A_{2B} receptor

activation: A mutational analysis of transmembrane domains 4 and 5 and the second

extracellular loop. *Purinergic Signal*. 8, 23–38

63   Peeters, M.C. *et al*. (2012) The role of the second and third extracellular loops of the

adenosine A_1 receptor in activation and allosteric modulation. *Biochem*. *Pharmacol*. 84,

76–87

64   Nguyen, A.T.N. *et al*. (2016) Role of the second extracellular loop of the adenosine A_1

receptor on allosteric modulator binding, signaling, and cooperativity. *Mol*. *Pharmacol*.

90, 715–725

65   Nguyen, a. T.N. *et al*. (2016) Extracellular loop 2 of the adenosine A_1 receptor has a key

role in orthosteric ligand affinity and agonist efficacy. *Mol*. *Pharmacol*. 90, 703–714

66   May, L.T. *et al*. (2007) Allosteric modulation of G protein–coupled receptors. *Annu*. *Rev*.

Pharmacol. *Toxicol*. 47, 1–51

67   Massink, A. *et al*. (2015) Sodium ion binding pocket mutations and adenosine A_{2A}

receptor function. *Mol*. *Pharmacol*. 87, 305–313

68   Gutiérrez-de-Terán, H. *et al*. (2013) The role of a sodium ion binding site in the allosteric

modulation of the A_{2A} adenosine G protein-coupled receptor. *Structure* 21, 2175–2185

69   Barbhaiya, H. *et al*. (1996) Site-directed mutagenesis of the human A_1 adenosine receptor:

influences of acidic and hydroxy residues in the first four transmembrane domains on ligand binding. *Mol. Pharmacol.* 50, 1635–1642

70   Dawson, E.S. and Wells, J.N. (2001) Determination of amino acid residues that are accessible from the ligand binding crevice in the seventh transmembrane-spanning region of the human A_1 adenosine receptor. *Mol. Pharmacol.* 59, 1187–1195

71   Gao, Z.-G. (2003) Identification of essential residues involved in the allosteric modulation of the human A_3 adenosine receptor. *Mol. Pharmacol.* 63, 1021–1031

72   Gao, Z.-G. *et al.* (2002) Structural determinants of A_3 adenosine receptor activation: Nucleoside ligands at the agonist/antagonist boundary. *J. Med. Chem.* 45, 4471–4484

73   Stoddart, L.A. *et al.* (2014) Effect of a toggle switch mutation in TM6 of the human adenosine A_3 receptor on G_i protein-dependent signalling and G_i-independent receptor internalization. *Br. J. Pharmacol.* 171, 3827–3844

74   Massink, A. *et al.* (2016) 5'-Substituted amiloride derivatives as allosteric modulators binding in the sodium ion pocket of the adenosine A_{2A} receptor. *J. Med. Chem.* 59, 4769–4777

75   Chen, A. *et al.* (2001) Constitutive activation of A_3 adenosine receptors by site-directed mutagenesis. *Biochem. Biophys. Res. Commun.* 284, 596–601

76   Liu, R. *et al.* (2014) A yeast screening method to decipher the interaction between the adenosine A_{2B} receptor and the C-terminus of different G protein alpha-subunits. *Purinergic Signal.* 10, 441–453

77   Dror, R.O. *et al.* (2009) Identification of two distinct inactive conformations of the β2-adrenergic receptor reconciles structural and biochemical observations. *Proc. Natl. Acad. Sci. U. S. A.* 106, 4689–4694

78   Beukers, M.W. *et al*. (2004) Random mutagenesis of the human adenosine A_{2B} receptor

followed by growth selection in yeast. Identification of constitutively active and gain of

function mutations. *Mol*. *Pharmacol*. 65, 702–710

79   Jazayeri, A. *et al*. (2017) Structurally Enabled Discovery of Adenosine A_{2A} Receptor

Antagonists. *Chem*. *Rev*. 117, 21–37

80   Bharate, S.B. *et al*. (2016) Discovery of 7-(Prolinol-N-yl)-2-phenylamino-thiazolo[5,4-

d]pyrimidines as novel non-nucleoside partial agonists for the A_{2A} adenosine receptor:

Prediction from molecular modeling. *J*. *Med*. *Chem*. 59, 5922–5928

81   Isberg, V. *et al*. (2015) Generic GPCR residue numbers – aligning topology maps while

minding the gaps. *Trends Pharmacol*. *Sci*. 36, 22–31

FIGURES LEGENDS

Figure 1: Overview of the structural sections of an adenosine receptor. Each section, further illustrated in panels I-III, is focus of a dedicate chapter within the text, describing key structural features of the adenosine receptor family: (I) The orthosteric binding site. (II$_A$) Allosteric modulation in the loop regions. (II$_B$) Allosteric modulation by sodium and amilorides. (III) The G protein binding site. The key residues in each section are shown according to a pseudo-sequence alignment of human adenosine receptor subtypes.

Figure 2. Orthosteric ligand binding (a) Topological overview of adenosine receptors, with the different regions of the orthosteric ligand binding site depicted and amplified in panels b-d. (**b**) The purine-derivative scaffold common to agonists and antagonists superimposes in the same binding region, as shown for agonist NECA in the active-like A$_{2A}$AR structure (blue) and the antagonist ZM241385 in complex to the inactive A$_{2A}$AR (orange). (**c**) Crystal structures of antagonist PSB-36 bound to A$_{2A}$AR (orange) and to A$_1$AR (magenta), highlighting residue 270^{7x34} (T/M/M/L), which has been identified as a key position involved in ligand selectivity. (**d**) Residues involved in agonist binding, shown for the agonist-bound A$_{2A}$AR structure in complex with NECA (blue, hydrogen bonds in dashed lines) and superimposed to the corresponding inactive structure of the same receptor (orange). An inward movement of helices in TM1, TM5, and TM7 is observed, resulting in a collapse of the sodium-binding pocket (see Figure 3). The table shows the effect of selected alanine mutations of the A$_{2A}$AR on binding (and potency) of the different pharmacological classes of orthosteric ligands. A detrimental effect is shown in red, while blue denotes an increasing effect.

Figure 3. Sites for allosteric modulation. (a) Topological overview of adenosine receptors, with the different regions involved in binding of allosteric ligands depicted and amplified in panels b-d. (**b**) Extracellular loops 1 and 2 from A_1AR (pink) and $A_{2A}AR$ (orange) crystal structures. The conserved disulfide bridge between TM3 – EL2 (positions C^{3x25} – C^{45x50}) and the $A_{2A}AR$ specific disulfide bridges in EL2 ($C71^{23x51}$– C159 and $C74^{3x22}$– C146) are shown in sticks. (**c**) The downward movement of residues $W246^{6x48}$ and $F242^{6x44}$, observed in agonist-bound structures of $A_{2A}AR$ (orange) and the fully active conformation in complex with a G protein mimic (green). This conformational change, which is related to the outward movement of TM6 characteristic of GPCR activation, is proposed to be hindered upon binding of the NAM amiloride and derivatives. (**d**) The sodium binding pocket, shown in complex with Na^+ as revealed in the $A_{2A}AR$ inactive structure (orange, hydrogen bonds in dashed lines). In agonist-bound structures, this pocket is collapsed because of a bulge in TM7 around residue $N284^{7.49}$, which is incompatible with the binding of Na^+, explaining the mechanism of sodium as NAM. This also applies for the fully-active, G-Protein mimic bound $A_{2A}AR$ structure (green). The table shows the effect of selected alanine mutations of the $A_{2A}AR$ on binding (and potency) of the different pharmacological classes of orthosteric ligands. A detrimental effect is sh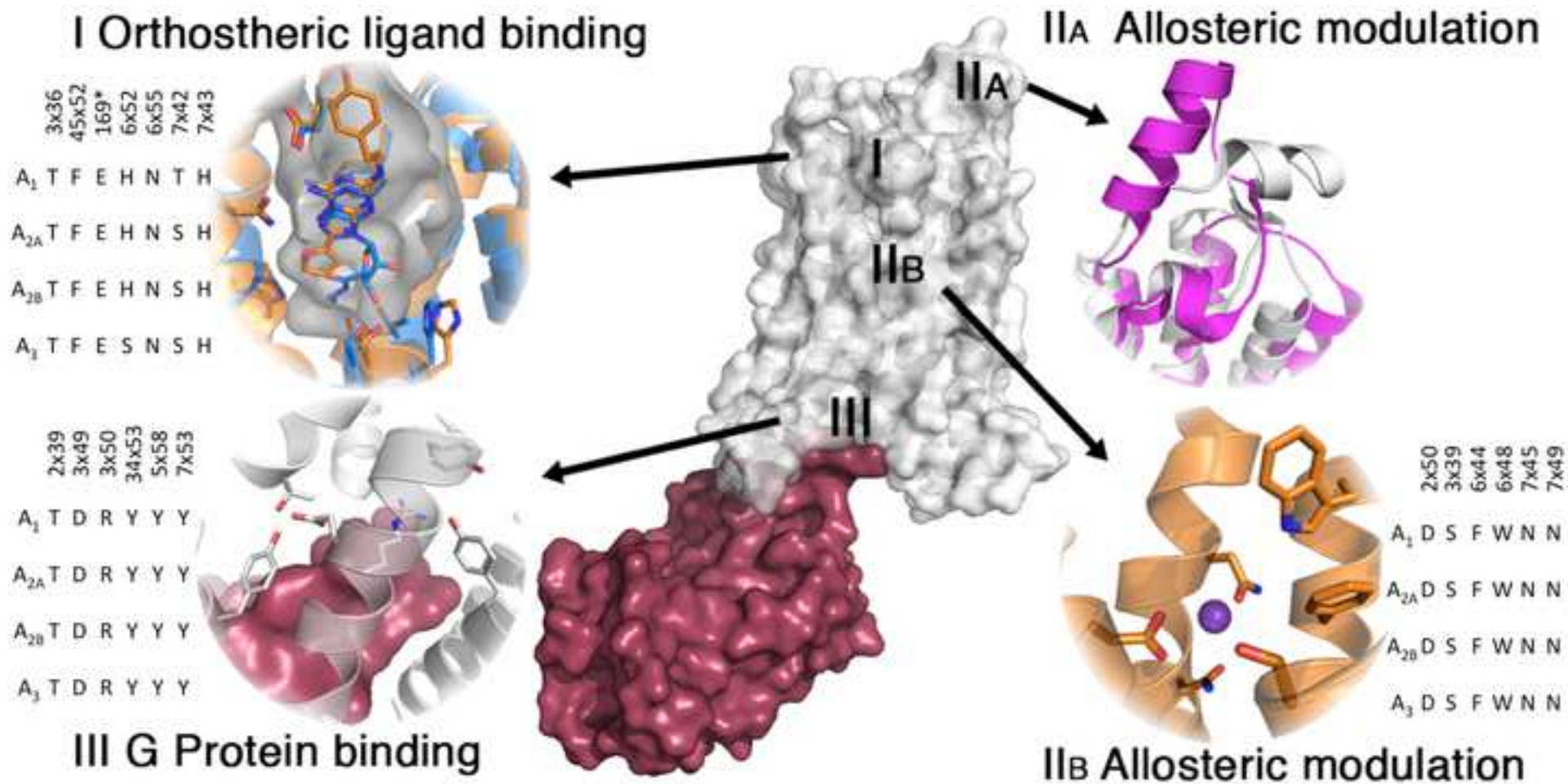own in red, while blue denotes an increasing effect. In both cases a high intensity of such effect (>30 fold) is depicted by a darker color. [a] There is only thermostability data available for F2426x44. [b] No measurable activation by agonists due to high basal activities. NE = no effect.
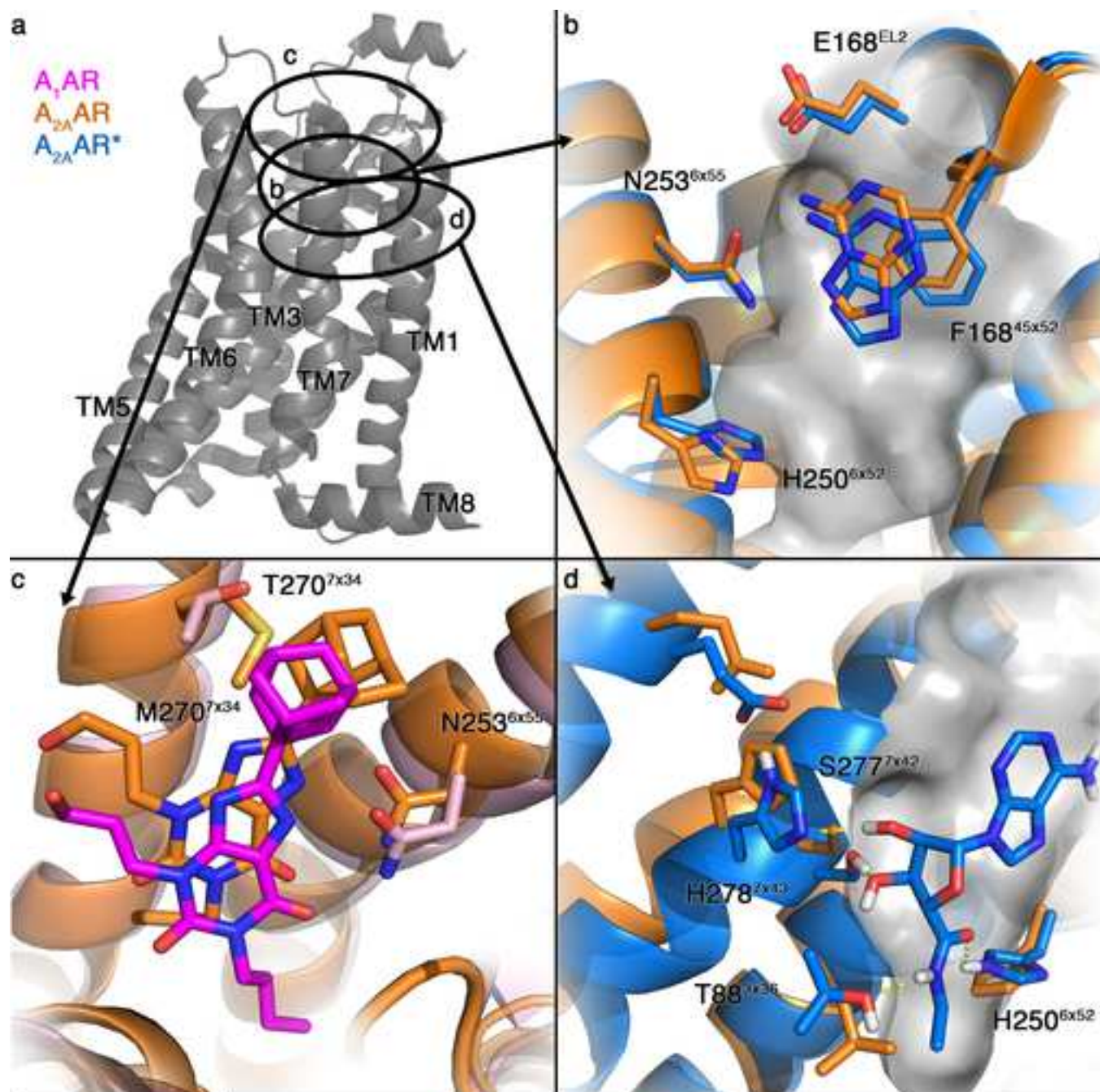
Figure 4. Receptor signaling and G protein binding. (**a**) Topological overview of adenosine receptors, with the different regions involved in receptor signaling and G protein binding depicted and amplified in panels b-d (color code as in figures 2 and 3). (**b**) Residues $Y197^{5x58}$ and $Y288^{7x53}$ form a possible activation switch, interacting in the G protein bound state (green), an interaction that is lacking in the inactive structures (orange), even if their orientation is somehow similar, while in agonist-bound structures without the G protein (blue) $Y197^{5x58}$ flips outwards in the membrane. (**c**) The interaction between $E228^{6x30}$ and the sidechain (ionic lock) or backbone or of $R102^{3x50}$ is observed in inactive $A_{2A}AR$ structures, in one case replaced by interaction of $E228^{6x30}$ with $R107^{3x55}$. (**d**) The TDY triad ($T41^{2x39}$-$D101^{3x49}$-$Y112^{34x53}$) form a 'cage' around $R102^{3x50}$ in inactive (orange) and agonist bound (blue) $A_{2A}AR$ crystal structures, blocking the access of the G Protein. Conversely, in the G protein-bound crystal structure (green), $R102^{3x50}$ is free and, according to the low density observed in the corresponding crystal structure (5g53), can be modeled to form a hydrogen bond to $Y197^{5x58}$ as shown in the panel. The table shows the effect of selected alanine mutations of the $A_{2A}AR$ on binding (and potency) of the different pharmacological classes of orthosteric ligands. (Color code as in Figures 2 and 3. [a] No data for $A_{2A}AR$, data from $A_{2B}AR$ (T^{2x39}, Y^{5x58})/A_3AR(Y^{7x53}, D^{3x49}). [b] No mutations to alanine, (-) no data, (NE) = no effect. [c] No $A_{2A}AR$ data, increased basal activities (E^{6x30}) or decreased potency (Y^{34x53}) in β_2

Figure I (for Box 2) Ligands co-crystallized with adenosine receptors. Chemical structures of agonists (upper row) and antagonists (middle and lower rows) co-crystallized with the ARs. Conserved interactions between receptor and both agonist and antagonist are attributable to the chemical motif denoted with a red square on each structure. Most antagonists also contain a purine core or an analogous heterobicycle, which are shown in blue.

Outstanding Questions Box

- Ligand selectivity between receptor subtypes can be achieved by exploiting sequence differences within the binding site (selectivity hotspots), but it also can be due to residues in the loop regions distal from the binding site. Additionally, the latest crystal structures revealed large conformational differences in both regions between adenosine receptors. To what extend do these structural properties contribute to ligand selectivity?

- The stereospecific ribose moiety is a characteristic feature of full agonists, while partial agonists have a mimic that is predicted to sit in the same binding site. Why do the same mutations in the ribose pocket have a different effect on full and partial agonists? Do these different classes of agonists maybe stabilize different intermediate receptor states?

- The activation pathway in class-A GPCRs seems to be quite conserved. Still, adenosine receptors present specific structural signatures related to agonist specific interactions and receptor activation: Is the TDY-triad a regulatory motif in the activation of adenosine receptors? How does the ribose trigger receptor activation?

- The residence time for a ligand can be quite different between receptor subtypes, and the mutagenesis and structural data suggest that ligand binding kinetics is controlled to a big extent by the extracellular loop region. What are the structural and dynamic determinants behind this control mechanism?

- There is direct structural evidence for a sodium binding site for allosteric modulation, and indirect (mutagenesis) evidence for a second site in the EL region. Will future crystal structures confirm the existence of this allosteric site? Can allosteric ligands modulate loop dynamics, thus affecting the residence time of orthosteric ligands?

Figure 1 (Key Figure)

I Orthostheric ligand binding

	3x36	45x52	169*	6x52	6x55	7x42	7x43
A_1	T	F	E	H	N	T	H
A_{2A}	T	F	E	H	N	S	H
A_{2B}	T	F	E	H	N	S	H
A_3	T	F	E	S	N	S	H

IIA Allosteric modulation

III G Protein binding

	2x39	3x49	3x50	34x53	5x58	7x53
A_1	T	D	R	Y	Y	Y
A_{2A}	T	D	R	Y	Y	Y
A_{2B}	T	D	R	Y	Y	Y
A_3	T	D	R	Y	Y	Y

IIB Allosteric modulation

	2x50	3x39	6x44	6x48	7x45	7x49
A_1	D	S	F	W	N	N
A_{2A}	D	S	F	W	N	N
A_{2B}	D	S	F	W	N	N
A_3	D	S	F	W	N	N

Figure 2 - revised

Click here to download Figure Figure_2-LZW.tif

Mutation	Partial agonist		Agonist		Antagonist
	Binding	Potency	Binding	Potency	Binding
E13A^{1x39}	-		-	NE	-
T88A^{3x36}	NE				
F168A^{45x52}	-		-		
E169A*	-	-		-	
H250A^{6x52}	-	-			
N253A^{6x55}	-			NE	
S277A^{7x42}			-	NE	
H278A^{7x43}	-	-			

Figure 3   Click here to download Figure Figure_3-LZW.tif ⬇
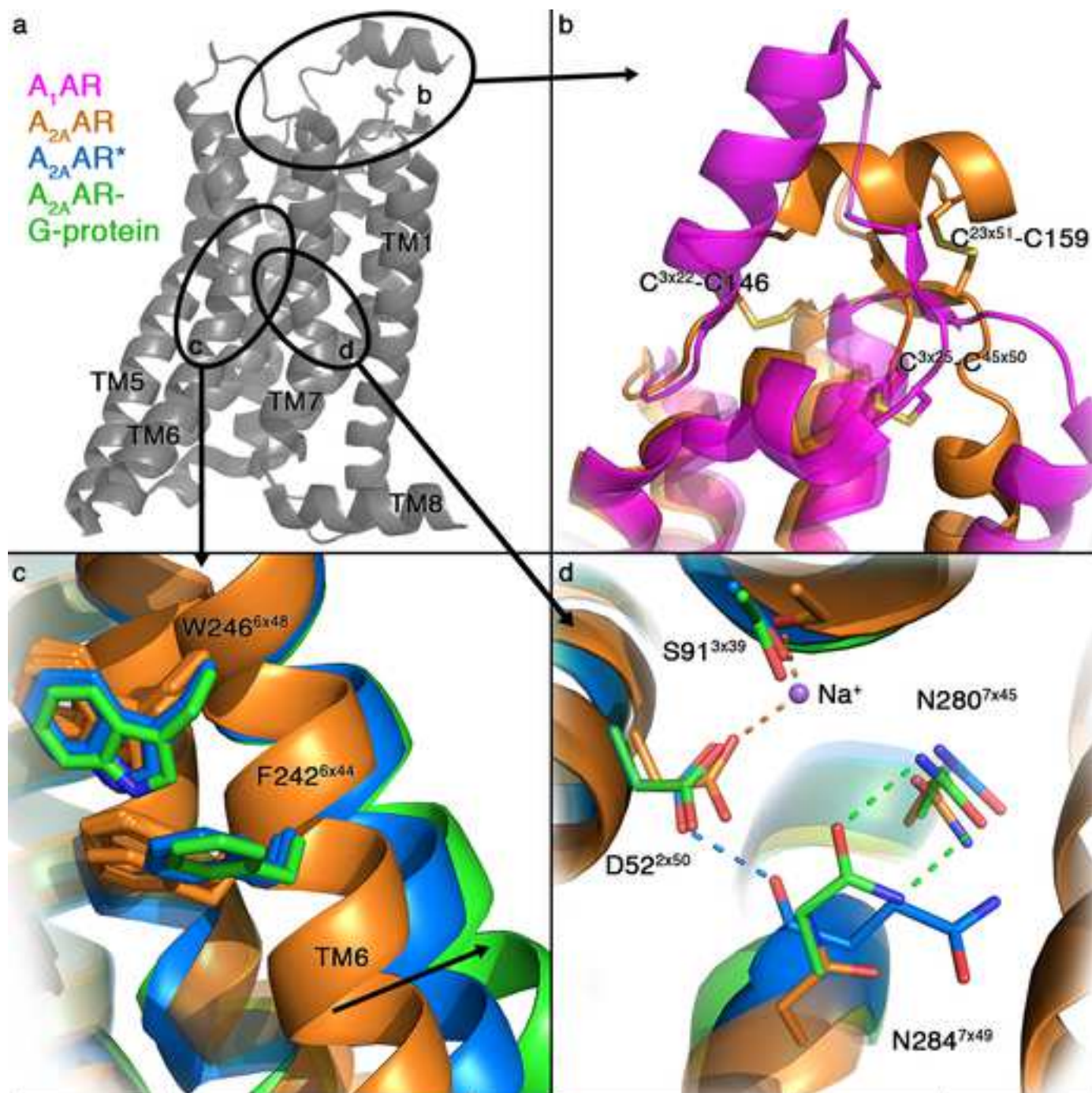
Mutation	Partial agonist		Agonist		Antagonist	Allosteric modulator
	Binding	Potency	Binding	Potency	Binding	Binding
D52A^{2x50}	-	-				
S91A^{3x39}	-	-		b		
F242A$^{6x44\ a}$	-	-	-	-	-	-
W246A^{6x48}						
N280A^{7x45}	-	-				
N284A^{7x49}	-	-	NE		NE	
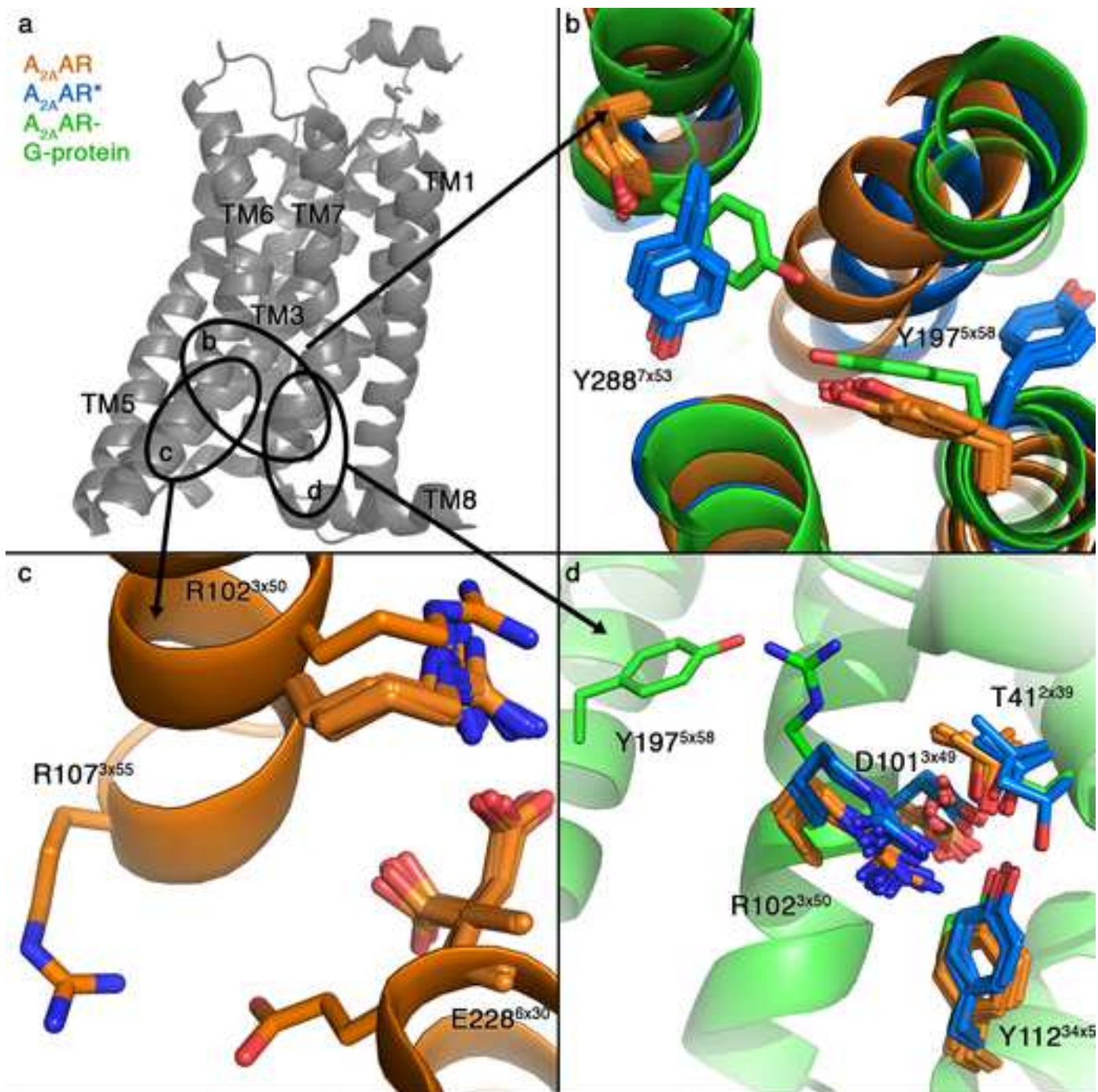
Mutation	Basal activity	Potency	Emax	Thermostability	
				Agonist	Antagonist
T41A[2z39]	🟦	-	-	-	-
D101A[3x49 a]	NE	NE	NE	-	-
R102A[3x50]	🟦	NE	NE	-	-
R107A[3x55]	-	-	-	-	🟦
Y112A[34x53 c]	-	-	-	-	-
Y197S/N[5x58 a,b]	🟦	-	-	-	-
E228[6x30 c]	-	-	-	-	-
Y288F[7x53 a,b]	NE	🟧	-	-	-

Figure I (for Box 2)

Adenosine

NECA

UK432097

CGS21680

Caffeine

XAC

DU172

PSB-36

ZM214385

T4G

T4E

8D1